SCIENTIFIC PAPER
Published: February 5, 2025
https://doi.org/10.13167/2025.30.1

A novel approach for improving seismic characteristics of coupled primary-secondary structural systems

Omid Fereidooni[1], Panam Zarfam[1] and Mohammadreza Mansoori[1]

[1] Islamic Azad University, Department of Civil Engineering, Science and Research Branch, Tehran, Iran

Corresponding author:
Panam Zarfam
zarfam@srbiau.ac.ir

Received:
May 19, 2024

Revised:
August 4, 2024

Accepted:
August 29, 2024

Published:
February 5, 2025

Citation:
Fereidooni, O.; Zarfam, P.; Mansoori, M.
A novel approach for improving seismic characteristics of coupled primary-secondary structural systems.
Advances in Civil and Architectural Engineering,
2025, 16 (30), pp. 1-23.
https://doi.org/10.13167/2025.30.1

ADVANCES IN CIVIL AND ARCHITECTURAL ENGINEERING (ISSN 2975-3848)

Faculty of Civil Engineering and Architecture Osijek
Josip Juraj Strossmayer University of Osijek
Vladimira Preloga 3
31000 Osijek
CROATIA

Abstract:
This study evaluates the primary-secondary structure interaction in three-dimensional single- and multi-story steel frame structures. A novel and practical approach was proposed to consider the effect of secondary systems. Additionally, a technique was developed to lower the time period of coupled structures. This is particularly helpful in high-rise buildings when exposed to earthquakes. Five types of steel frames were designed, fabricated, and subjected to seismic loading. The experimental models were exposed to ground motion excitations and the finite element models were subjected to nonlinear dynamic time-history analyses. An excellent agreement between the two approaches were observed. According to the results, infill wall displacements and accelerations were considerably reduced by utilizing the deformable wall setting. In this regard, the story displacements and accelerations decreased from 209 to 211 mm and 17,8 to 18,0 meter per square second when secondary systems were used. In addition, free vibrations of the frames were considerably reduced when the concentrated mass secondary systems were implemented.

Keywords:
primary-secondary structure interaction; three-dimensional steel frame; seismic behaviour; numerical modelling; infill wall; wall post

1 Introduction

Secondary systems are elements attached to the floors, walls, and roofs of a building or facility, which are typically not designed or intended for load bearing. However, these systems can sustain large seismic forces and depend on their structural characteristics to resist loads. Secondary systems are generally classified into three broad categories: (i) building, (ii) architectural, and (ii) mechanical/electrical components. The structural characteristics of secondary systems, including mass, stiffness, and damping, differ from those of the primary structure and do not contribute to the gravity and lateral load-bearing capacity of the coupled structure. However, secondary systems are subjected to earthquake loading, which can cause their failure. Damage to secondary structures can also pose significant safety risks, prevent the functioning of buildings, or lead to major economic losses. Therefore, the characteristics of these structures should be appropriately addressed to maintain the efficiency of the entire system during and after earthquakes.

One of the most important parameters in the analysis of coupled structures is the primary-secondary structure interaction (PSSI). In this regard, the entire system reacts as a compound structure, with simultaneous vibrations in both systems. Thus, the dynamic responses of the primary and secondary systems affect one another. Consequently, eliminating PSSI from the modelling process will lead to inaccurate results. PSSI is typically more effective in the response of secondary structures, particularly when more than one secondary structure is connected to a primary companion. Therefore, the effect of PSSI multiplicity complicates the analysis of the structural response, which is generally neglected to simplify design codes. Without considering PSSI in the analysis of secondary structures, inaccurate estimates of the response of secondary structures are usually obtained.

Structural walls comprise the most common secondary systems in frame structures. In contrast, non-structural walls are those surrounding the building or those separating the interior space. The investigation and design of such components are highly significant because debris from these walls causes considerable financial and human losses during earthquakes. Accordingly, the enforcement of measures to restrain wall debris has been considered in most countries and included in seismic or executive regulations. For instance, the sixth appendix of the Iranian Seismic Standard 2800, titled "Seismic Design and Implementation of Non-Structural Architectural Components," was announced in 2018. This code considers the implementation of wall posts as a constraint to significantly reduce the seismic failure of the surrounding and separating walls. However, this code overlooked the connection of these components to primary structures and the existence of enclosed walls inside these constraints, which cause response interference between the primary structure and secondary system that bears weight and exhibits stiffness. Therefore, this performance interference or the resulting interaction should be considered in the seismic behaviour of an entire structure. Globally, the issue of designing non-structural components against earthquakes was first raised in 1978 by Applied Technology Council (ATC) 03-06 [1], in which a method for calculating the earthquake load was prescribed, after which the topic was included in the ensuing regulations. Subsequently, the seismic design of secondary structures was contained within Chapter Thirteen of the American society of civil engineering (ASCE) 7-05 [2] under the title of "Seismic Design Requirements for Non-Structural Components." However, the methods and relationships presented in the technical literature for analysing secondary systems are complex. Nonetheless, very few investigations have been conducted to simplify the analysis methods, which may be due to the complexity of the governing equations or the numerous parameters that affect the structural response. Singh et al. [3] presented simple relationships for analysing secondary systems. Although the relationships were of good logical and theoretical support, they were not sufficiently simple to be included in the regulations for wide use. In line with Singh et al. [3], Chen and Soong [4] presented relationships that formed the basis of the National Earthquake Hazards Reduction Program (NEHRP) 1995 recommendations [5-8]. These relationships not only led to significant developments in design codes, but also suggested several parameters for calculations that had not been considered

before. Villaverde [9-13] also proposed simple relationships for analysing secondary systems. In the relationships provided by Villaverde, the nonlinear behaviour of secondary systems is included via the response reduction factor. This method is considered a major improvement upon international codes.

Numerous studies have addressed the performance characteristics of coupled structures. For instance, Adam [14] experimentally examined the actual response of secondary systems with frequencies close to those of the primary structure. In another study, Filiatrault and Sullivan [15] revealed that coupled structures could exhibit low performance levels owing to the failure or collapse of non-structural systems. However, further experimental investigations are required to better understand the behaviour of these systems. Accordingly, a simple floor response (FRS) spectrum was proposed to assess the behaviour of non-structural components [16, 17]. This approach computes the maximum response of the secondary system using the primary structure response spectrum. Subsequently, Ghafory-Ashtiani and Fayouz [18] proposed a technique for estimating the responses of secondary systems in two forms: static equivalent and spectral analysis. Kazantzi et al. [19] investigated strength reduction factors in the design of non-structural components, providing estimated relationships for the coupled system response. The seismic demand for non-structural elements in frame structures was evaluated by Chalarcal et al. [20]. Recently, Torkian and Khodakarami [21] used incremental dynamic analysis to estimate the damage to structures with infill walls. Bangoli et al. [22] conducted a state-of-the-art review addressing the literature studies and design problems of systems with infilled walls. Sakacli et al. [23] introduced a new generation of infill wall blocks and investigated the effects of these secondary systems on single-span steel-frame structures. It was concluded that adding these wall types to steel frames increased the base shear, energy dissipation, and rigidity by 64-68 %, 50-62 %, and 25-40 %, respectively. Jagadeesan et al. [24] used infilled walls in reinforced concrete frames to improve structural performance. Wang et al. [25] proposed a new infilled frame with an improved flexible connection to mitigate the detrimental infill-frame interactions via the arching effect. Asteris [26] proposed a new FE technique for analysing infilled plane frames under lateral loading, investigating the effect of the infill panel opening on the reduction in frame stiffness. They showed that the shear force redistribution was critically affected by the presence and continuity of the infill panels, where the presence of infill decreased the shear forces in the columns. Yekrangnia and Asteris [27] suggested a model for masonry-infilled frames with openings that could accurately consider the nonlinearity of frame structures. A comprehensive review was conducted by Dias-Oliveira et al. [28] regarding the lessons learned from recent earthquakes and the evolution of structural codes by considering infill masonry panels.

Secondary systems are unavoidable structural components that affect the seismic performance of coupled structures. However, PSSI has frequently been disregarded in codes used in practice and thus requires further investigation. This study numerically and experimentally examined the seismic characteristics of three-dimensional (3D) multistory moment-resisting frame structures with and without infill walls and restraining wall posts. Accordingly, five types of steel frames were fabricated and subjected to ground motion recording in the experimental program using a shake table. In addition, finite element (FE) coupled frame models were created using Structural Analysis Program (SAP) 2000 software. The numerical results were also confirmed using the FE Abaqus software. The models were exposed to a set of seven earthquake records obtained from the Pacific Earthquake Engineering Research (PEER-NGA) and scaled for nonlinear dynamic time-history analysis. It was revealed that the secondary systems noticeably increased story displacements despite their very light weight, altering the seismic behaviour of the entire system. However, in the structures with deformable wall seating, the subsequent displacements were considerably reduced, and the input earthquake energy in these structures quickly dissipated. Free vibration of the coupled frames was eliminated when the devised concentrated mass secondary systems were used in the steel frames.

2 Methodology

2.1 Model configuration

This section describes the properties of the test-frame models investigated in this study. The 3D moment-resisting frame structures with one, two, and three floors were constructed in the laboratory at the Crisis Management and Infrastructure Engineering Center of Urmia University, Iran. Each frame comprised four perimeter columns and beams, which were regarded as primary structures (see Figure 1). The beams and columns were box sections with cross-sectional dimensions of 60 × 60 × 4 mm. Additionally, the floors were made of 5-mm-thick steel plates with dimensions of 150 × 150 mm and material specifications similar to those of other steel materials.

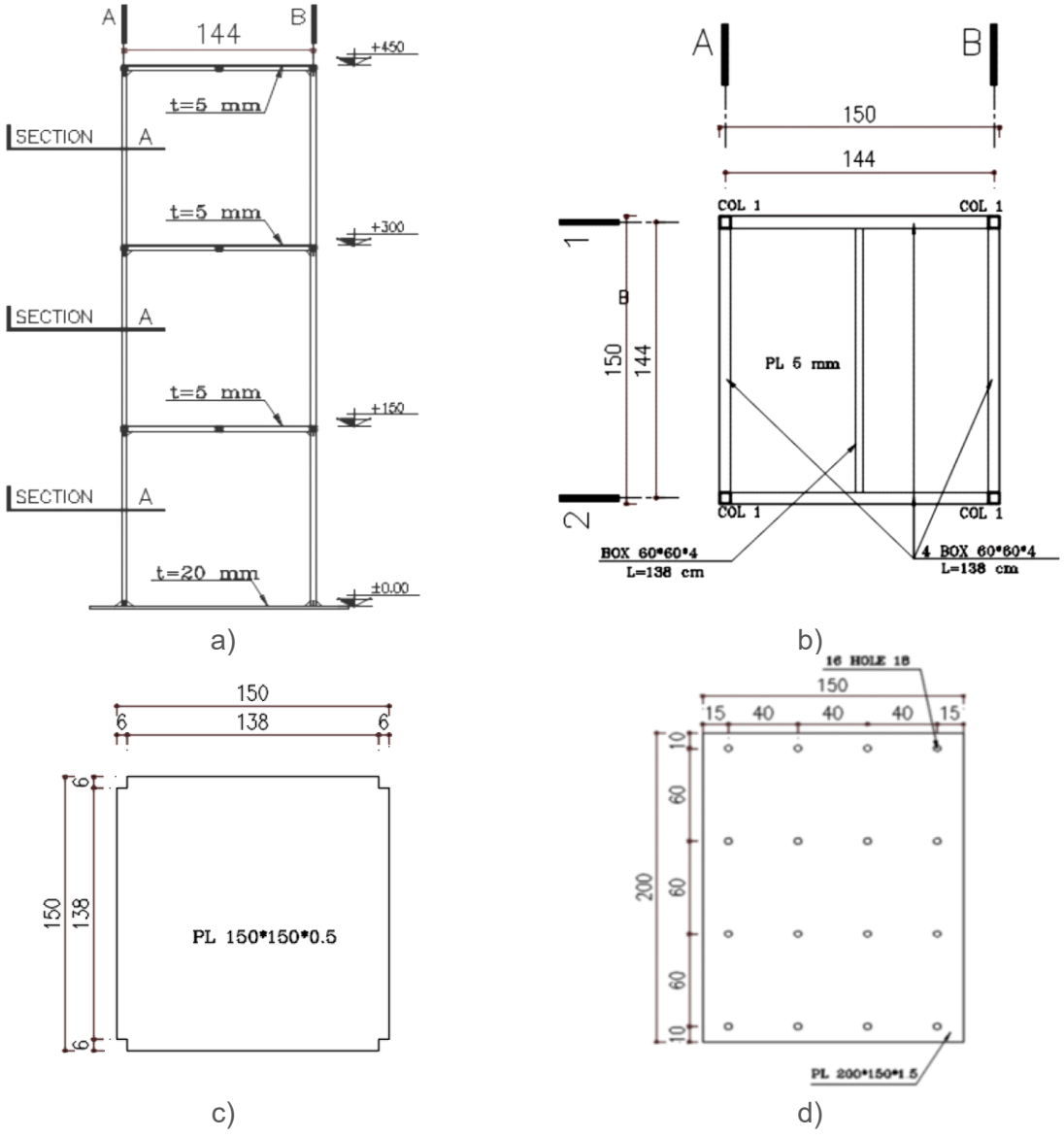

Figure 1. Geometric details of a three-story experimental frame model: (a) elevation, (b) plan, (c) floor plate, and (d) base plate

The height and span of each story along the three axes were 1500 mm. Furthermore, reinforcing bars with lengths 250 mm and diameters of 6 mm were attached to the primary

system and used to model the secondary systems with an overall mass of less than 20 % of that of the primary system, following the code requirements (ASCE) 7-05 [2].
The secondary system also comprised 9 mm thick perimeter walls built with bricks and four wall posts at each story with lengths of 138 mm and an angled section with dimensions of L 20 × 20 × 2 mm. The entire coupled system was bolted to a shaking table using a plate with dimensions of 2000 × 1500 × 15 mm. Figure 1 demonstrates the geometric details of the three-story experimental model and corresponding components built in this investigation.
To conduct the experiments in this study, the shaking table implemented in the laboratory was a single-degree-of-freedom system with a rate of 250 mm/s. The dimensions of the table were 2000 × 3000 mm. The shake table can simulate two types of harmonic and ground motion loadings. The maximum weight capacity of this device was 2,5 tons and the maximum acceleration that could be produced was 3,5 g; where g denotes the ground acceleration. The maximum displacement is 300 mm. Two types of sensors and a data logger were used to measure and record the motion of the coupled structure and shaking table. Three accelerometers were implemented in this system, one of which was installed as the table accelerometer to control the input accelerogram applied to the structure. The second accelerometer was attached to the first floor of the primary system and the third was placed on the secondary system located on the first floor. In addition, three linear variable differential transformers (LVDTs) were used as displacement measurement devices and mounted on the side of the coupled structure at the level of each floor in a lateral fixture position. The side structure was built with the required strength to withstand the movements of the structure and to create a suitable system for varying motions. The data logger used in this experiment was fabricated using Rayan sensors with 16 input ports. This device can simultaneously record 20 data points per second from different transducers, including the force, displacement, strain, and acceleration. The investigated parameters and the entire procedure of data collection, observation, and storage were adjusted using SoftLogger software. Figure 2 shows the details of the accelerometers, LVDTs, data loggers, and SoftLogger software screens. A schematic of the test setup is shown in Figure 3.

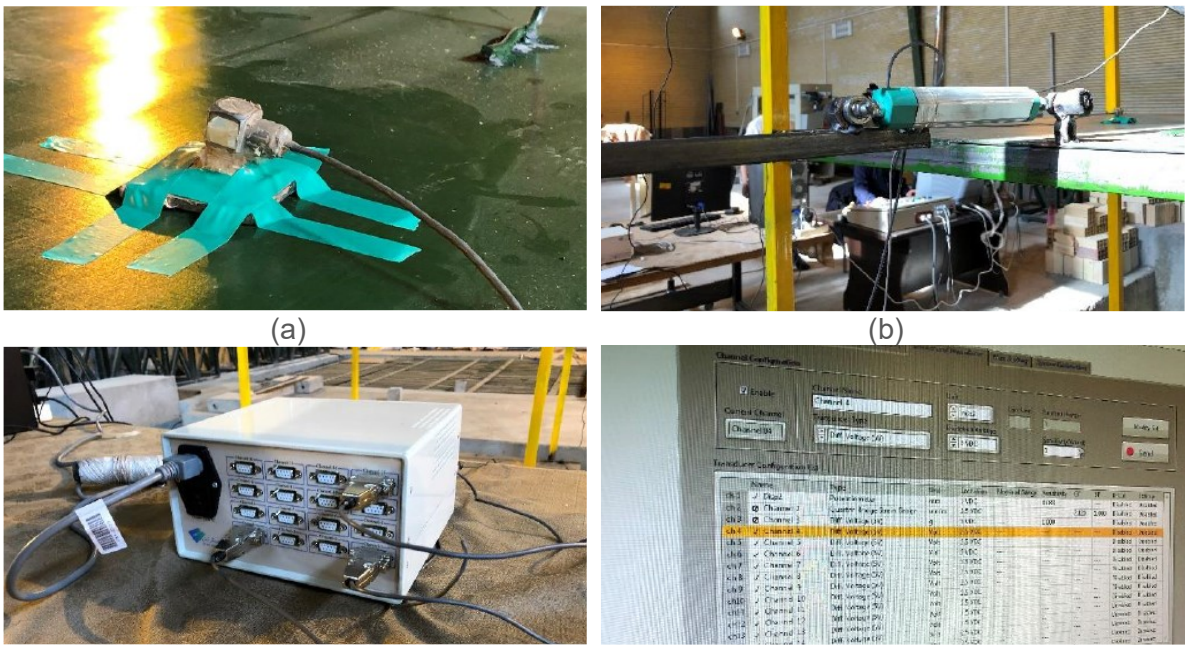

Figure 2. Details of the (a) accelerometers, (b) LVDTs, (c) data logger, and (d) SoftLogger software screen

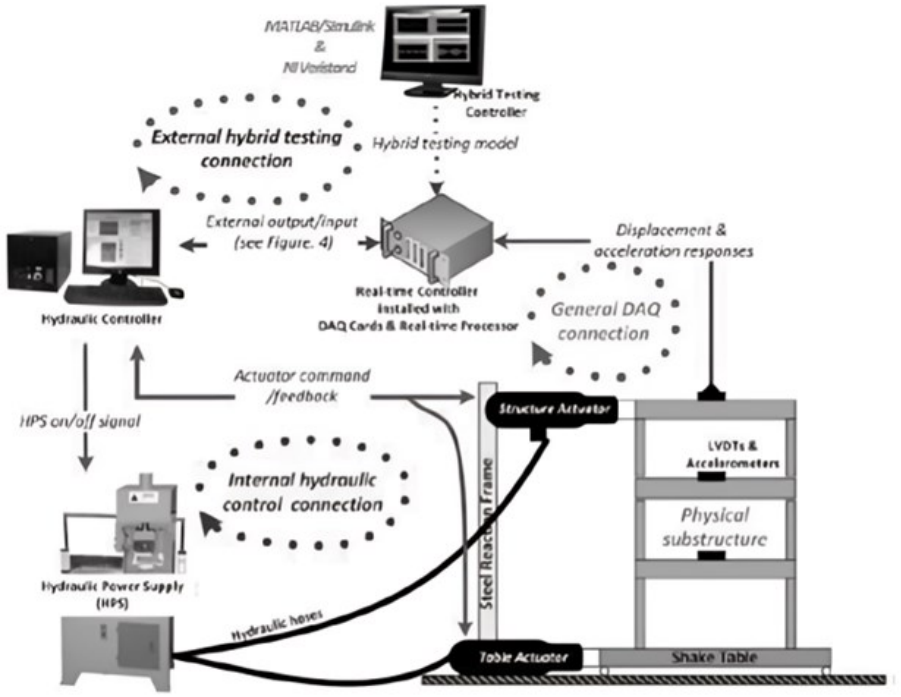

Figure 3. Schematic of the entire experimental setup

In addition, to model secondary systems with single supports, a novel hypothetical element that expresses the stiffness of the secondary system was proposed. This element was designed with a height of 250 mm and a circular shape fabricated in the laboratory with Φ 6 mm reinforcing bars and welded to the primary structure at floor levels in desired locations for investigation. To model the mass of the secondary system, a concentrated mass was provided at the end of the rebar by welding a metal piece with a certain weight. In addition, the wall posts were welded to the primary structure at the half span of each floor. Figure 4 shows the configuration of the primary moment-resisting frame model and the attached secondary systems.

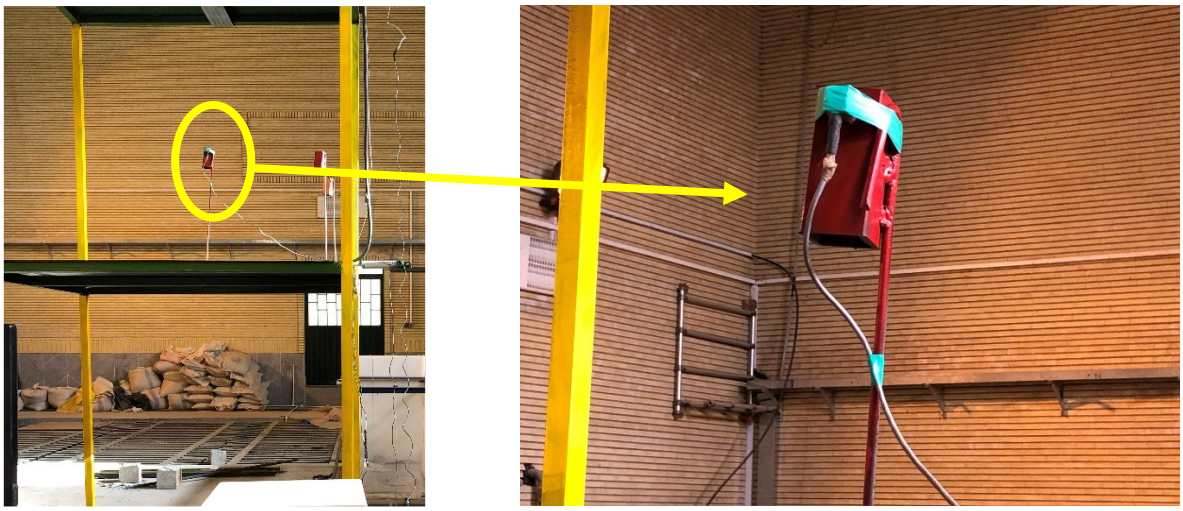

a) b)

Figure 4. Configuration of the (a) primary moment-resisting frame model and (b) secondary attached system

In this study, five types of 3D two-story frame structures were designed, fabricated, and subjected to seismic excitations. The first type included a primary frame without walls, wall posts, or concentrated masses. The second type included no walls or wall posts, but three concentrated masses were as integrated as secondary systems on the first floor. The locations of the attached concentrated masses are explained in detail in Section 3. The third type of two-story coupled system included six concentrated mass compartments, three of which were placed on the first floor and three on the second floor. Furthermore, the fourth type of coupled system comprised 3D primary frames accompanied by perimeter brick walls and associated wall posts installed at the corners and mid-spans on the second story with no concentrated mass. The second floor was selected for implementing the brick wall based on the premise that the placement of secondary systems with certain time periods at a specified height produces a better performance in reducing the response of the entire coupled structure. The walls were connected to the floor with an epoxy adhesive to model the conventional wall-floor connection. In addition, the wall posts did not continue up to the end of the wall, and a gap was created based on code recommendations. The fifth type of structure was similar to the fourth type, except that the wall was built over a deformable base on the floor. This deformability was achieved by placing a rubber sheet on the floor before building a wall. We aimed to examine the effect of a deformable layer beneath the secondary walls on the seismic performance of the entire coupled structure. The results for each system type are discussed in Section 4. The details of each frame type are shown in Figures 5a to 5h.

Figure 5. Representation of five types of 3D two-story frame structures: (a) Type I, (b) Type II, (c) Type III, (d) wall post-frame connection, (e) Type IV, (f) Type IV wall-frame connection, (g) Type V, (h) Type V wall-frame connection

2.2 Loading of coupled structure

The process of selecting and scaling seismic records is next explained. The accelerogram corresponding to the Kobe earthquake was selected as the input record for application to a scaled structure in the laboratory. Given that the scale factor of the experimental model in this study was 1:3, the time parameter of this record was scaled by 1/3, and the acceleration parameter had a scale factor of 3 in the Seismosignal software [29]. Figures 6a and 6b show the scaled Kobe excitation acceleration and displacement graphs, respectively. These graphs were input to the SoftLogger software for application to the coupled system through the shaking table.

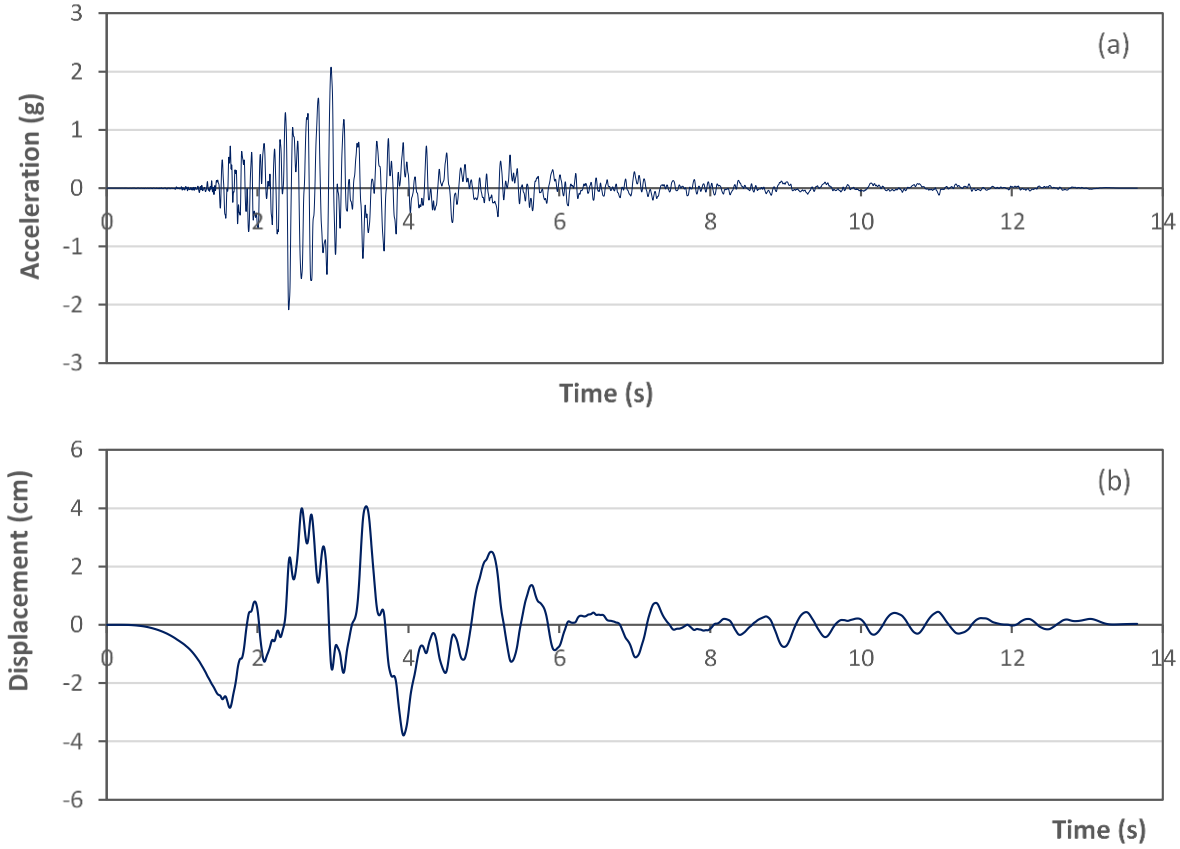

Figure 6. Scaled Kobe earthquake excitation (a) acceleration and (b) displacement graphs

3 Numerical Modelling

3.1 Configuration of FE models

This section describes the configurations of the numerical models created using SAP2000. Accordingly, the experimental frames built in the laboratory were modelled using the FE approach. Thus, 3D coupled frame structures with one, two, and three stories were created using SAP200 software version 19 [30]. In these models, the height of each story was 4500 mm and the span lengths along the two horizontal axes were 4500 mm. The four perimeter columns and beams were composed of box sections with dimensions 180 × 180 × 12 mm. To achieve the required system period, each floor was modelled using a 15 mm thick steel plate with a middle beam at the midspan to avert the out-of-plane buckling of the floor plate. All connections were considered fixed during the modelling procedure. For the secondary system, wall posts were selected from two angle cross sections with dimensions of 2L 60 × 60 × 6 mm at the face of each column and four 4L 60 × 60 × 6 mm at the mid-spans to constrain the

perimeter brick walls with a thickness of 270 mm. In addition, to model secondary systems with single supports, a bar element with a lump mass at its end was modelled to simulate the stiffness and mass of the secondary system. This element was designed with a height of 750 mm and a varying circular cross-section. To achieve a wide range of secondary systems with different stiffnesses and an overall mass of less than 20 % of that of the primary system, five different cross sections of the bars were considered: Φ 18, Φ 30, Φ 42, Φ 54 and Φ 60. This was selected to conduct a more extensive investigation on the seismic behaviour of secondary systems. Accordingly, these systems were denoted as SS-1, SS-2, SS-3, SS-4, and SS-5.
Considering the height of each structure, the structures under investigation were ensured to be within the range of systems with low or medium time periods whose seismic behaviour lies within the maximum scope of the seismic spectrum response. Therefore, the dimensions and weights of the structures were chosen such that the period of the primary structures was in the range of 0,15-0,70.
Three locations were designated on each storey floor to mount the concentrated mass secondary system. The first point was assumed to be at the corner of the floor, the second point was at the centre of the lateral axes perpendicular to the direction of the earthquake, and the third point was presumed to be at the centre of each floor. Figures 7a, 7c, and 7e show the locations of these points in each frame story. The notation of these points was such that 1 was assigned to the corner point, 2 to the side point, and 3 to the central point of the single-story coupled structures. Similarly, the locations of the secondary systems were determined on the second floor as numbers 4, 5, and 6, and numbers 7, 8, and 9 were used as the secondary system locations on the third floor. Figures 7b, 7d, and 7f present three-dimensional views of the structural models with the attached secondary systems.

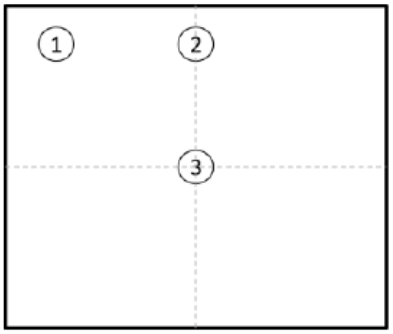

a)

b)

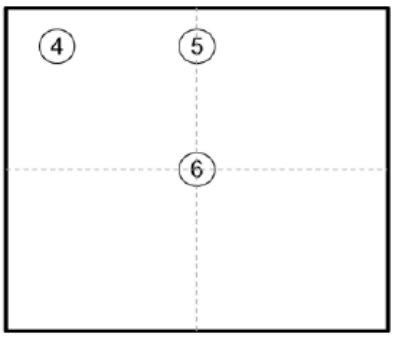

c)

d)

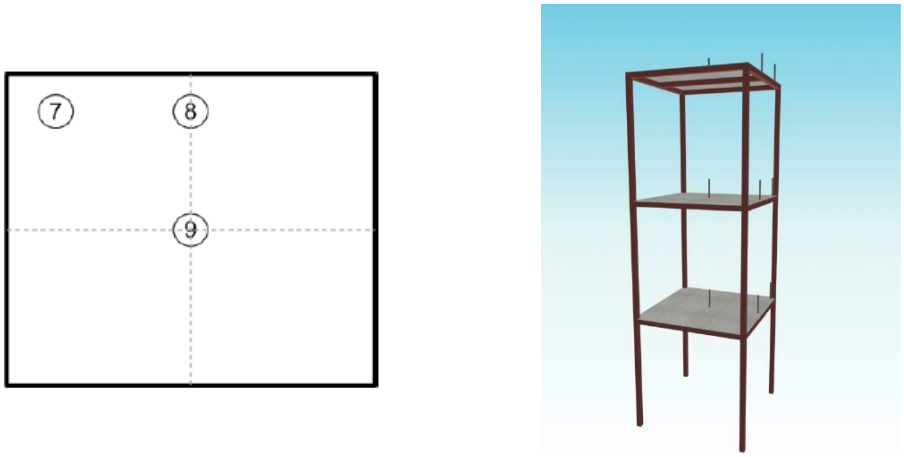

e) f)

Figure 7. Schematics of secondary system location and geometry for the (a) and (b) first floor; (c) and (d) second floor; (e) and (f) third floor

3.2 Loading of the FE models

The loading of coupled systems can be categorised into two parts: primary and secondary structures. The primary structures are subjected to vertical and lateral loads. In cases where secondary systems were attached to the primary systems, the lateral loading of the primary structure, in terms of seismic acceleration, was automatically applied. The loading related to the secondary systems was also exerted separately according to the type of secondary system, which is a type of vertical gravity load. The vertical load applied to the primary structure was also of the gravity type. However, considering the nature of this study, this load was not divided into live and dead loads. Once the loading was characterised in SAP2000, the analysis steps were defined. In this regard, time-history analysis was chosen as the most reliable analytical method available for the dynamic analysis of structures, which calculates the responses of the structure over time increments under the influence of the input ground motion record. Subsequently, a set of seven earthquake records obtained from PEER-NGA were chosen and scaled according to the ASCE7-16 requirements to signify an extensive sort of amplitude. Table 1 presents the characteristics of the input earthquake records in the SAP2000 software.

Table 1. Characteristics of the input earthquake records

No.	Ground Motion			Lowest Frequency (Hz)	PGA (g)	PGV (cm/s)
	Magnitude	Year	Name			
1	6,7	1994	Northridge	0,25	0,52	63
2	7,1	1999	Duzce	0,06	0,82	62
3	6,9	1995	Kobe	0,13	0,51	37
4	7,3	1992	Landers	0,13	0,42	42
5	6,9	1989	Loma Prieta	0,13	0,53	35
6	7,4	1990	Manjil	0,13	0,51	54
7	7,6	1999	Chi-Chi	0,05	0,51	39

Each secondary system was tied to the frame floor at different locations on each story in various configurations, as shown in Fig. (8). Table 2 lists the scale factor of each ground motion record in the preliminary analysis step of the modelling using SAP2000 software.

Table 2. Scaling factors for the selected earthquake records

No.	Ground Motion	Scale Factor
1	Northridge	0,7941
2	Duzce	1,0405
3	Kobe	0,6996
4	Landers	0,6406
5	Loma Prieta	0,6509
6	Manjil	1,0971
7	Chi-Chi	1,0171

It should be noted that regarding the record selection, Moeindarbary and Taghikhani [31] stated that the optimal design parameters in maximum considered earthquake (MCE), design basis earthquake (DBE), and service level earthquake (SLE) systems are similar in specifications, and therefore, hazard levels play insignificant roles in the record selection process. A nonlinear dynamic time-history analysis was adopted to compare the seismic responses of the coupled structures with those of the experimental program, the results of which are discussed in “Section 4”.

To verify the numerical analysis procedure, the authors also implemented an alternative FE software, ABAQUS, in the modelling procedure. In this respect, the steel material was ordinary structural steel with an elastic modulus of 200 GPa, yield stress of 240 MPa, and Poisson’s ratio of 0,3. In addition, a bi-linear model featuring a strain-hardening capacity was applied to simulate the nonlinear and inelastic properties of the steel material. As such, the plastic strain varied from a yield strain of 0,6 to the ultimate strain. The wall material was modelled as brick tiles with an elastic modulus of 1448 MPa, compressive strength of 2,5 MPa, and Poisson’s ratio of 0,3. Concrete damage plasticity (CDP) was used to model the fracture behaviour of the bricks. All the modelled primary and coupled frame structures were initially examined through modal analysis, and the associated fundamental periods were accurately computed using software. Similar results were obtained using both software programs. Table 3 summarises the secondary system time periods versus variations in the mass ratio (ɣ).

Considering the complexity of the dynamic relationships between primary and secondary systems, design codes neglect the effects of the interaction between these systems, and secondary systems are only applied as an additional mass on the primary structure. Therefore, in the numerical part of this study, we attempted to provide a simple design technique for calculating the fundamental period of a coupled system considering the multiplicity of secondary systems. This was performed to overcome the previous research gap by developing and simplifying existing dynamic relationships. Consequently, the fundamental period of the coupled structure was used to replace the period of the primary structure in the seismic design relationships.

Three types of interaction effects of secondary systems on the seismic behaviour of primary structures can be selected. In the first case, it is assumed that the secondary systems behave independently; thus, the interaction effects of the secondary systems on the seismic behaviour of the primary and coupled systems are ignored. In the second case, to apply the interaction, all primary and secondary systems are modelled together as a coupled system, and analysis and design are on this basis. However, in the third case, which is proposed in the present study, it is possible to combine the above two cases by doing more experimental works. Consequently, by modelling the structure for the first case and to apply the significant interaction effects regarding the seismic behaviour of the primary structure, several corrective relationships were suggested in this study. A methodology for a coupled system period was proposed. Therefore, two approaches were adopted to consider the secondary systems. First, only the primary structure was modelled by applying the weight of the secondary system, which is referred to as mass modelling in this study. Second, all primary and secondary systems were modelled in the form of a coupled system, hereafter referred to as system modelling.

According to the seismic code recommendations, the maximum mass ratio of the secondary system to the primary structure was set to 20 % such that the interaction effects could be ignored. Therefore, in this study, the mass ratio was selected for 13 different cases according to Table 3, in compliance with the design code recommendations. The secondary mass was applied to the primary structure in mass modelling, as well as to the ends of all secondary systems attached to the five structural types described in the experimental program, that is, SS-1 to SS-5, during system modelling.

Table 3. Specifications of secondary system forces and the subsequent time periods

M_s	γ	T_s				
		SS-1	**SS-2**	**SS-3**	**SS-4**	SS-5
0	0,00	0,000	0,000	0,000	0,000	0,000
80	1,67	0,648	0,234	0,120	0,073	0,060
160	3,34	0,916	0,330	0,169	0,103	0,083
240	5,02	1,121	0,404	0,207	0,125	0,102
320	6,69	1,294	0,466	0,238	0,144	0,117
400	8,36	1,447	0,521	0,266	0,161	0,131
480	10,03	1,585	0,571	0,292	0,177	0,143
560	11,70	1,712	0,617	0,315	0,191	0,155
640	13,38	1,830	0,659	0,337	0,204	0,165
720	15,05	1,941	0,699	0,357	0,216	0,175
800	16,72	2,046	0,737	0,376	0,228	0,185
880	18,39	2,146	0,773	0,394	0,239	0,194
960	20,06	2,241	0,807	0,412	0,249	0,202

In the next step of the modelling process, secondary system forces were applied to the primary structure in two cases. In the first case, where mass modelling was considered, the secondary systems were removed, and the above forces were applied as weights on the roof levels of the primary structure. A schematic of the mass modelling approach for different frame structures is shown in Figure 8.

Figure 8. Schematic of the primary mass modelling approach for frames

In the second case (i.e., system modelling), the secondary systems were modelled along with the primary frame system and secondary forces were applied as weight forces at the end of the secondary systems. A schematic of the system modelling approach for different frame structures is shown in Figure 9.

Figure 9. Schematic of the secondary system modelling approach for frames

The loading of the peripheral walls and wall posts was investigated in this study. In addition to the PSSI, the difference in the seismic behaviour of the coupled system in the two cases of wall and wall post implementation on both conventional and deformable seating was modelled, similar to the experimental models built in the laboratory. Therefore, five system types were considered: (i) primary structure without a secondary system; (ii) primary structure with three secondary systems on the first floor; (iii) primary structure with six secondary systems on the first and second floors; (iv) primary structure with walls and wall posts on the second floor on conventional seating; and (v) primary structure with walls and wall posts on deformable seating. The comparison results between the experimental program and the FE analysis are presented in the following section.

4 Results and Discussion

In this section, the results obtained from the experiments are compared with those estimated by the numerical analysis. Because 20 data points were recorded per second by the data logger in the experimental section, the time interval between each point was 0,05 s. Therefore, the FE results obtained from SAP2000 were recorded every 0,05 s to obtain an accurate comparison of the results between the two modelling approaches in the four investigated PSSI states.

4.1 Results comparison of primary structure without secondary system

Figure 10 presents a comparison of the experimental and numerical analysis results for the two-story (2ST) frame system. For a better comparison, the maximum responses in the two analysis graphs are highlighted with dashed lines in both the positive and negative ranges. Based on the results, excellent agreement was observed between the two approaches. In this regard, Fig. 10a illustrates that the displacement variation of the first floor in system 2ST in the numerical analysis was 160,85 mm, whereas the corresponding measurement in the experimental system was 150 mm. This indicates a discrepancy of 7,95 % in the obtained results. Furthermore, Figure 10b shows the second-floor displacement in the 2ST frame in both the numerical and experimental analyses, where the maximum displacement responses were 211 and 231 mm, respectively, indicating a discrepancy of 9,55 % between the results.

Similarly, the variations in first-floor acceleration with time are shown in Figure 10c. The maximum accelerations in both the numerical and experimental analyses were 18,0 and 18,4 m/s^2, indicating a negligible difference of 2,04 % between the results.

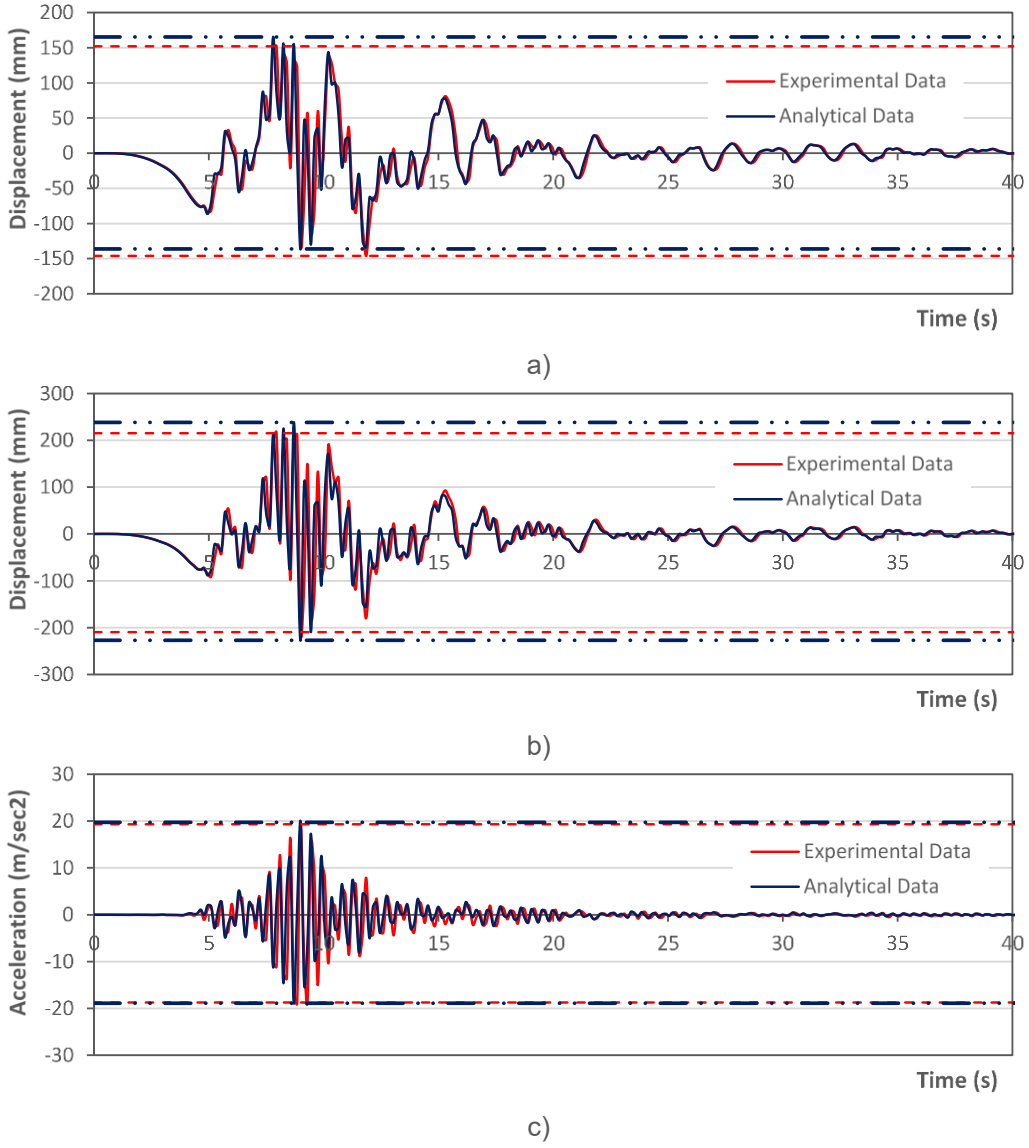

Figure 10. Comparison of results between the experimental and numerical analyses for the 2ST system: (a) first-floor displacement, (b) second-floor displacement, and (c) first-floor acceleration

4.2 Results comparison of the primary structure with three secondary systems

A comparison of the experimental and numerical analysis results for the two-story three-secondary system (2ST-3SS) frame structure with the three secondary systems on the first floor is shown in Figure 11. The maximum responses in the two graphs are highlighted by the dashed lines in both the positive and negative ranges. Based on the results presented in Figure 11a, the experimental result of the first floor displacement was 8,09 % lower than the numerical estimate, which were 150 and 162 mm, respectively. The second-floor displacements in the 2ST-3SS frame in both the experimental and numerical analyses are presented in Figure 11b. There was a difference of 9,72 % between the obtained results, and the maximum second-floor displacements in the 2ST-3SS frame were 209 and 229 mm. Similarly, Figure 11c shows the variations in the first-floor acceleration versus time in the 2ST-3SS frame. It is shown that

the maximum experimental and numerical accelerations were 17,80 and 18,08 m/s^2, indicating a slight difference of 1,62 % between these results. The variations in the secondary system acceleration are shown in Figure 11d. The corresponding values for the experimental and numerical analyses were 10,55 and 10,20 m/s^2, corresponding to a difference of 3,44 %.

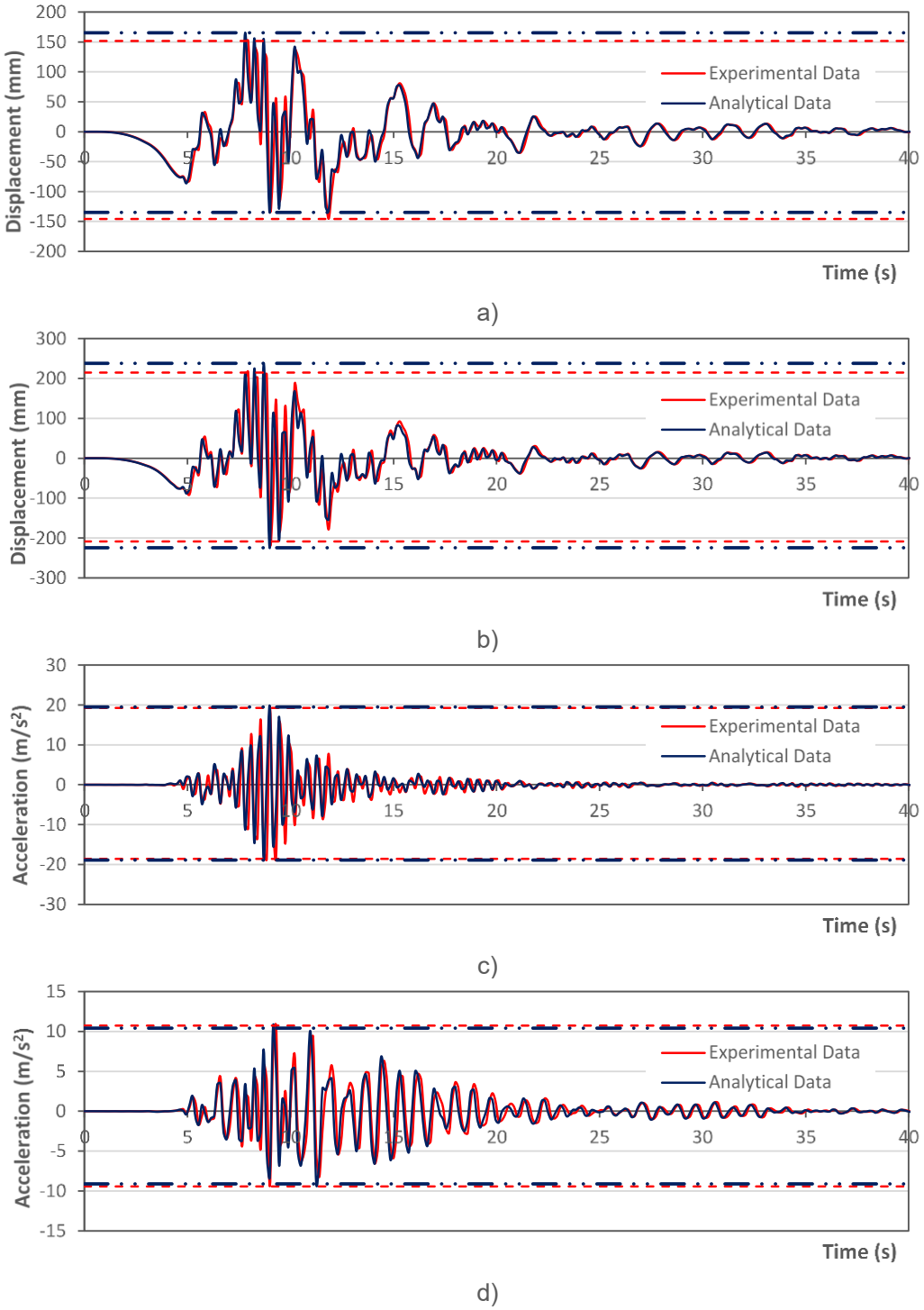

Figure 11. Comparison of results between the experimental and numerical analyses for the 2ST-3SS system: (a) first-floor displacement, (b) second-floor displacement, (c) first-floor acceleration, and (d) secondary-system acceleration

4.3 Results comparison of a primary structure with six secondary systems

Figure 12 presents a comparison of the experimental and numerical analysis results for the 2ST-6SS frame system. The maximum responses in the two analysis graphs are highlighted with dashed lines in both the positive and negative ranges. According to the results, there was good agreement between the two approaches. Figure 12a shows that the displacement variation of the first floor in system 2ST-6SS in the numerical analysis was 167 mm, whereas the corresponding measurement in the experimental system was 150 mm, corresponding to a small discrepancy of 9,4 % in the obtained results. Furthermore, Figure 12b shows the second-floor displacement in the 2ST-6SS frame for both the experimental and numerical analyses, where the maximum displacement responses were 211 and 231 mm, respectively, indicating a discrepancy of 10,39 % between these results. Similarly, the variations in first-floor acceleration with time are shown in Figure 12c. The maximum accelerations in both the experimental and numerical analyses were 18,2 and 19,0 m/s^2, indicating a negligible difference of 4,41 % between the results. The variations in the secondary system acceleration are shown in Figure 12d. The corresponding values for the experimental and numerical analyses were 10,48 and 11,00 m/s^2 with a maximum difference of 5,06 %.

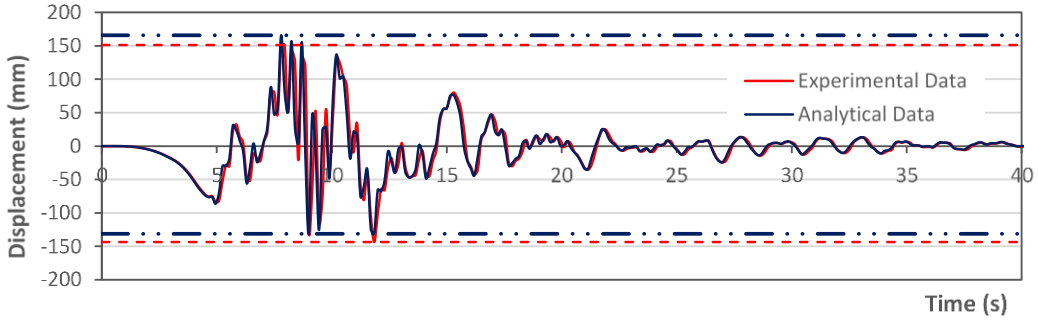

a)

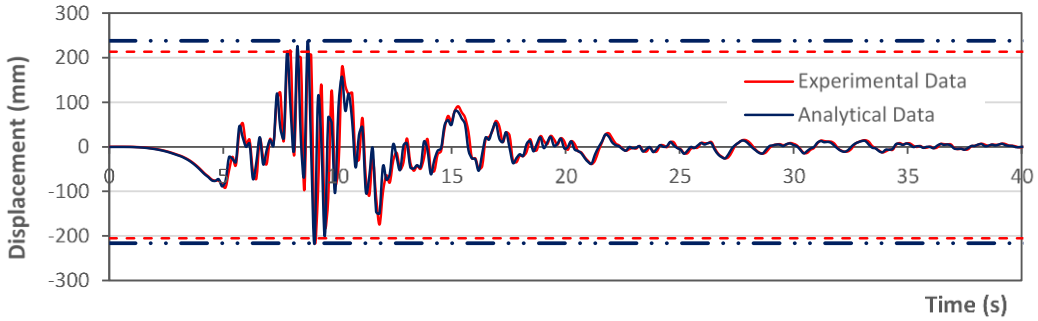

b)

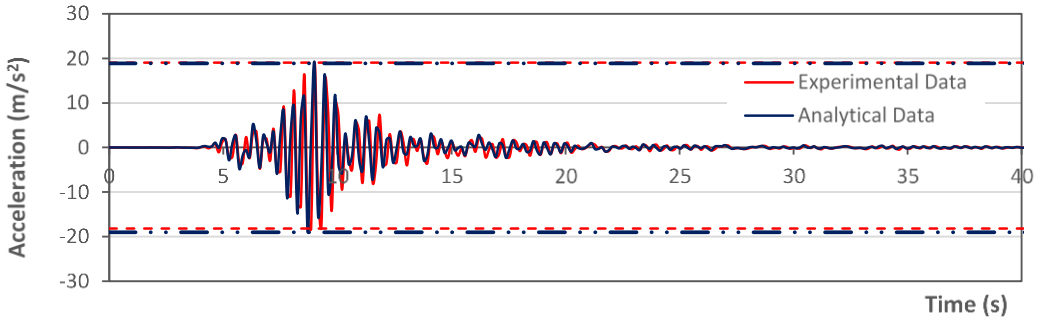

c)

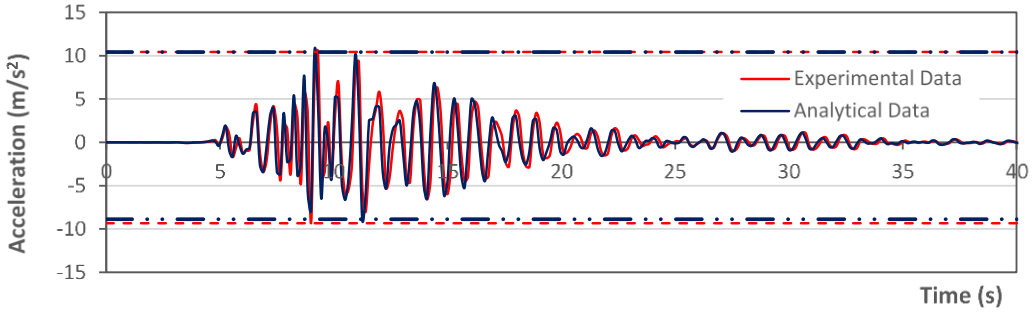

d)

Figure 12. Comparison of results between the experimental and numerical analyses for the 2ST-6SS system: (a) first-floor displacement, (b) second-floor displacement, (c) first-floor acceleration, and (d) secondary-system acceleration

4.4 Results comparison of the primary structure with a wall and wall post on a conventional seating on the second floor

A comparison of the experimental and numerical analysis results for the two-story frame structure with wall (2ST-WALL) and wall posts on a conventional seating on the second floor is shown in Figure 13. The maximum responses in the two graphs are highlighted by dashed lines in both the positive and negative ranges. Figure 13a shows that the experimental result was 13,21 % lower than the numerical estimate, which were 137 and 155 mm, respectively. The second-floor displacements in the 2ST-WALL frame in both the experimental and numerical analyses are presented in Figure 13b. A difference of 16,09 % was observed between the results, and the maximum second-floor displacements in the 2ST-3SS frame were 195,0 and 226,4 mm. Likewise, Figure 13c shows the variations in the first-floor acceleration over time in the 2ST-WALL frame. The maximum experimental and numerical accelerations were 7,60 and 8,14 m/s^2, corresponding to a slight difference of 7,07 %. The margin of discrepancy increased in this case compared to that in previous cases. This can be attributed to the implementation of brick walls, variations in wall weight, and a lack of mortar between the brick layers.

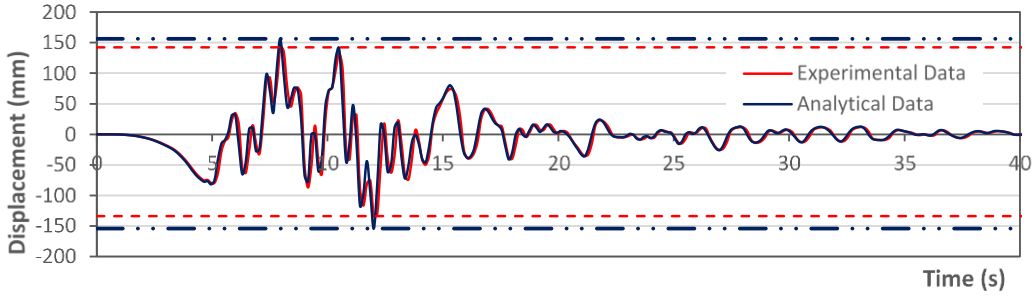

a)

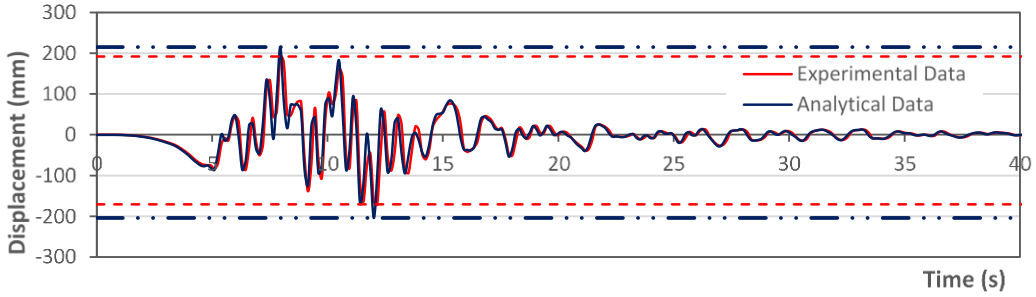

b)

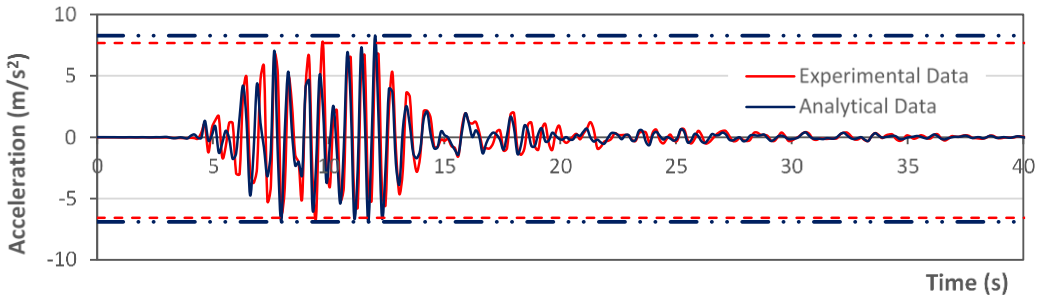

c)

Figure 13. Comparison of results between the experimental and numerical analyses for the 2ST-WALL system: (a) first-floor displacement, (b) second-floor displacement, and (c) first-floor acceleration

4.5 Results comparison of the primary structure with a wall and wall post on a deformable seating on the second floor

As explained previously in “Section 2”, to examine the idea of lowering the time period of coupled structures proposed in the current study, a rubber sheet layer was placed under the brick wall to act as deformable seating, and the experiment was performed on the 2ST-WALL system type. A comparison of the results obtained via the FE model is provided in Section 4.7 between the two types of coupled systems with conventional and deformable seating, denoted as 2ST-WALL and 2ST-WALL-P, respectively.

4.6 Interpretation of results for structures with 0, 3, and 6 secondary systems

The difference in the displacements of the first and second floors of the coupled structures with three and six secondary systems compared to the primary structure without any secondary system is shown in Figures 14a and 14b. In addition, the difference in the acceleration of the first floor of the coupled structures with three and six secondary systems compared to the primary structure without any secondary system is shown in Figure 14c.

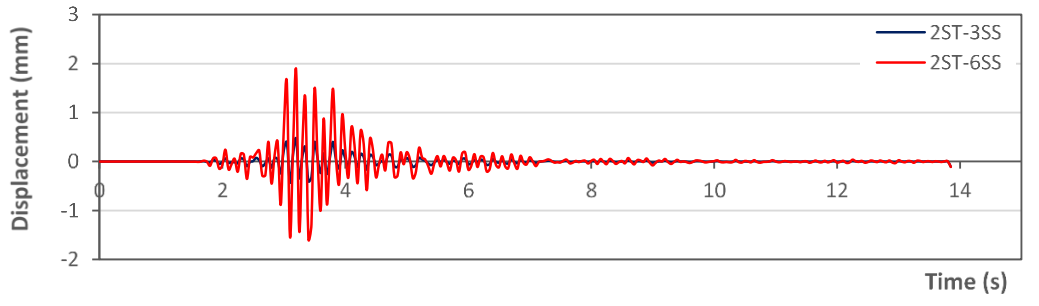

a)

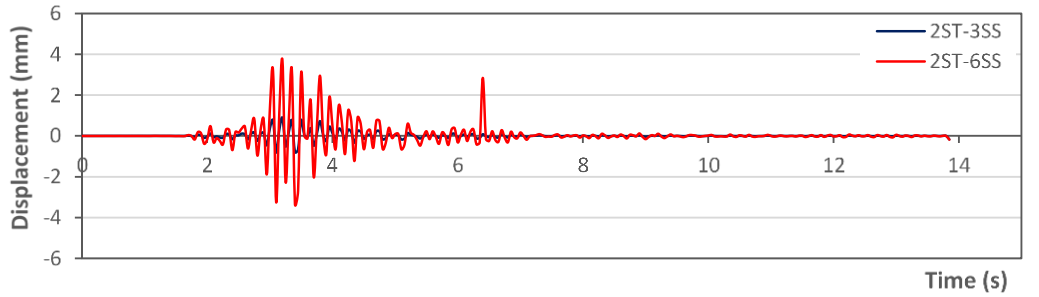

b)

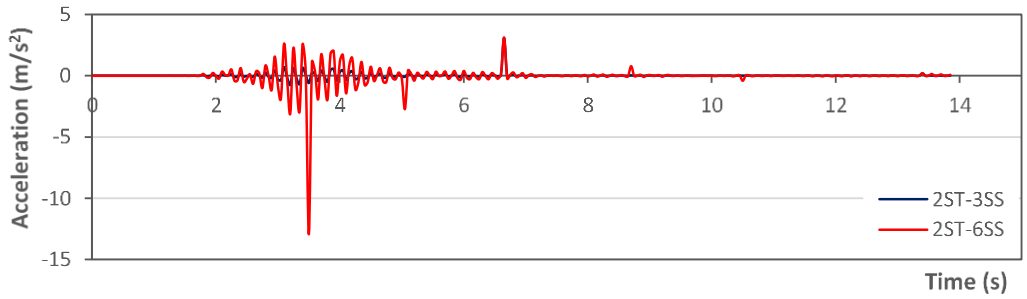

c)

Figure 14. Comparison of the results between structures with three and six secondary systems compared to the primary structure: (a) first-floor displacement, (b) second-floor displacement, and (c) first-floor acceleration

Although the secondary systems used in this study are much more lightweight than the primary structure, the increase in the displacement of the floors with the addition of these secondary systems was clearly observed. In particular, when using six secondary systems, the displacement increased up to 4 mm at the laboratory scale and to 12 mm at the real-world scale. This observation indicated that the period of the coupled system was changed by the attachment of these secondary systems. The obtained results clearly show that, by increasing the weight of the secondary system that it is properly connected to the primary structure, the period of the coupled system can significantly alter the seismic behaviour of the entire system. Interestingly, the experiments showed that in frames with secondary systems, the oscillation of the secondary systems was strong during excitation, and at the end of the experiment, the vibration of the primary structure finished very quickly while the secondary systems continued to freely vibrate. However, when testing primary structures without secondary systems, the primary structure continued to exhibit noticeable free oscillations after the completion of the excitation. This observation confirms that the periods of structures with longer periods can be conveniently reduced by designing similar secondary systems to improve their seismic responses.

4.7 Interpretation of the results of frames with conventional and deformable wall seatings

A comparison of the results between the structures with conventional and deformable wall seating regarding the displacement of the first and second floors and the acceleration of the first floor is presented in Figure 15. It is shown that structures with deformable-wall seating have lower displacements than those with conventional seating, although the difference in the maximum displacement is not significant. However, in structures with deformable wall seating, the subsequent displacements after the maximum values were considerably reduced, and the sudden seismic motions disappeared from the graphs. Therefore, the input earthquake energy in these structures dissipated quickly, and the structure returned to its normal state much faster. This indication is evident in the acceleration diagram of the first floor, signifying an appropriate seismic response of the structure. This finding proves that by implementing a simple deformable seat beneath the wall without any special measures, the period of the coupled structure can be changed and its seismic behaviour can be enhanced, indicating the benefits of this approach. Identifying suitable materials for use in deformable seating could be a topic of investigation in future research.

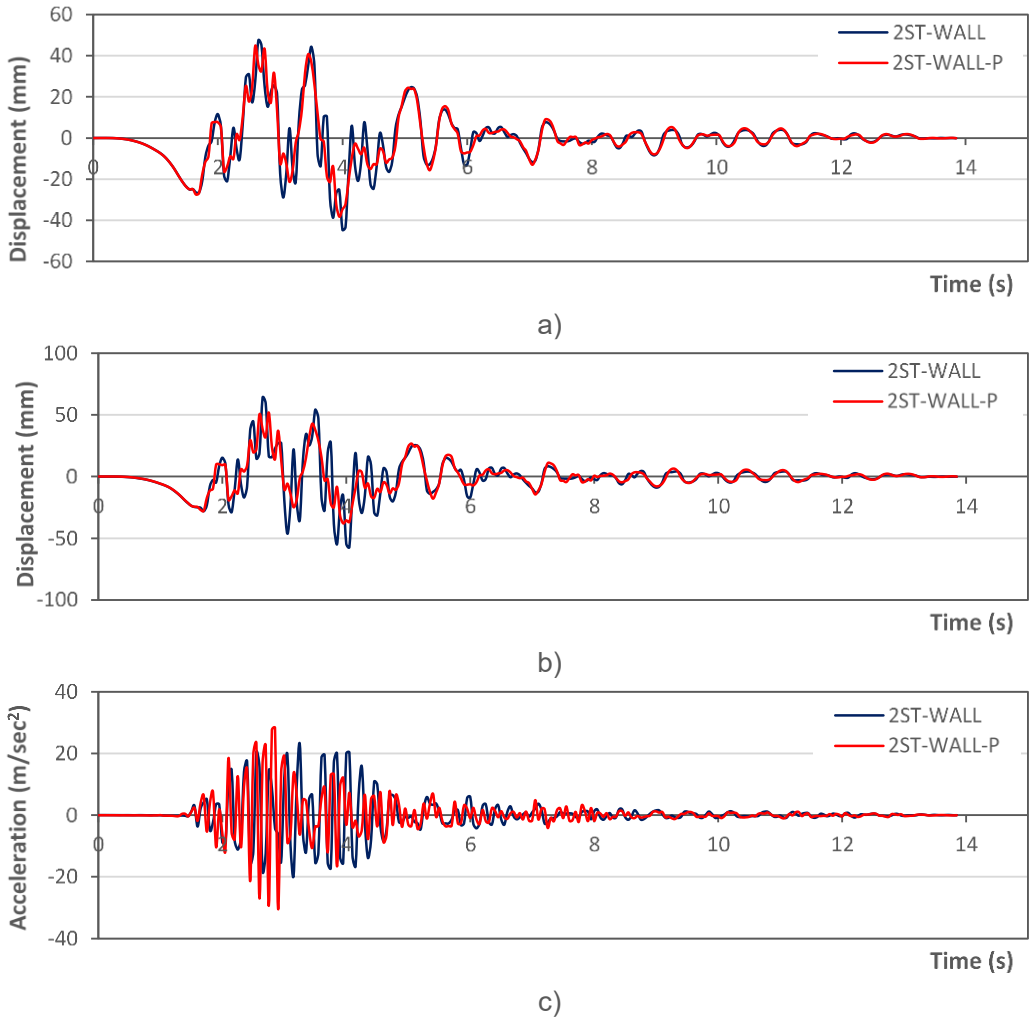

Figure 15. Comparison of the results of structures with conventional and deformable wall seating: (a) first-floor displacement, (b) second-floor displacement, and (c) first-floor acceleration

In general, good agreement between the experimental and numerical results was observed. This agreement was better observed in the acceleration diagrams than in the displacement graphs, which may be due to the high accuracy of the accelerometer sensors compared with the LVDTs that were used. In addition, the installation arrangement of the accelerometers compared with LVDTs may affect the obtained results. Although the vibration of the side structure for the connection of LVDTs was largely controlled, small vibrations that are uncontrollable in practice may have also contributed to the observed differences. Furthermore, the mismatch of the actual dimensions with the modelled dimensions and possible uncertainties owing to the mechanical characteristics of the materials may have contributed to the observed errors.

5 Conclusions

This study examined the effects of secondary systems on 3D steel frame structures. Five types of steel frames were designed, fabricated, and subjected to seismic loads. Experimental and numerical investigations were conducted to assess the seismic characteristics of the coupled primary-secondary structural systems. The experimental models were exposed to selected ground motion excitations, and the numerical models were subjected to a nonlinear dynamic time-history analysis. The following conclusions were drawn based on the obtained results:

- The story displacements changed from 209 to 211 mm and the accelerations decreased from 17,8 to 18,0 m/s^2 when the secondary systems were used.
- An increase in the displacement of the frame floors was observed with the addition of the proposed secondary system.
- The period of the coupled structure significantly altered the seismic behaviour of the entire system by increasing the weight of the secondary system.
- The secondary system successfully mitigated the free vibrations of the primary system. However, the secondary system sustained its vibrations following the completion of the seismic excitation.
- In structures with deformable wall seating, the displacements obtained after the maximum values were considerably reduced, and the input earthquake energy in these structures quickly dissipated.
- The presence of peripheral walls increased the period of the coupled structure. However, the use of a deformable layer beneath the wall at the floor level reduced the period and enhanced the seismic performance of the coupled system.

Abbreviations

3D	three-dimensional
ASCE	American Society of Civil Engineering
ATC	Applied Technology Council
CDP	Concrete Damage Plasticity
DBE	Design Basis Earthquake
FE	Finite Element
FRS	Simple Floor Response
LVDT	Linear Variable Differential Transformer
MCE	Maximum Considered Earthquake
NEHRP	National Earthquake Hazards Reduction Program
PEER-NGA	Pacific Earthquake Engineering Research
PGA	Peak Ground Acceleration
PGV	Peak Ground Velocity
PSSI	Primary-Secondary Structure Interaction
SAP	Structural Analysis Program
SLE	Service Level Earthquake
SS	Secondary Structure
T_s	secondary system time period
γ	secondary system mass ratio
Φ	rebar number

References

[1] US Department of Commerce, National Bureau of Standards. Applied Technology Council. ATC 3-06. *Tentative Provisions for the Development of Seismic Regulations for Buildings: A Cooperative Effort with the Design Professions, Building Code Interests, and the Research Community*. USA: ATC; 1978.

[2] American Society of Civil Engineers. ASC 7-05. *Minimum Design Loads for Buildings and Other Structures*. USA: ASCE; 2005.

[3] Singh, M. P.; Suarez, L. E.; Matheau, E. E.; Maldonado, G. O. Simplified Procedures for Seismic Design of Nonstructural Components and Assessment of Current Code Provisions. National Center for Earthquake Engineering Research, 1993.

[4] Chen, Y.; Soong, T. T. Seismic response of secondary systems. *Engineering Structures*, 1988, 10 (4), pp. 218-228. https://doi.org/10.1016/0141-0296(88)90043-0

[5] Building Seismic Safety Council for the Federal Emergency Management Agency. Nonbuilding structure design requirements - Report No. FEMA 302. In: *NEHRP Recommended Provisions for Seismic Regulations for New Buildings and Other Structures*. USA: Building Seismic Safety Council; 1997, pp. 223-254.

[6] Building Seismic Safety Council for the Federal Emergency Management Agency. Commentary - Nonbuilding structure design requirements - Report No. FEMA 303. In: *NEHRP Recommended Provisions for Seismic Regulations for New Buildings and Other Structures*. USA: Building Seismic Safety Council; 1997, pp. 199-222.

[7] Building Seismic Safety Council for the Federal Emergency Management Agency. Architectural, mechanical, and electrical components (Simplified and Systematic Rehabilitation) - Report No. FEMA 273. In: *NEHRP Guidelines for the Seismic Rehabilitation of Buildings*. USA: Building Seismic Safety Council; 1997, pp. 11/1-11/31.

[8] Building Seismic Safety Council for the Federal Emergency Management Agency. Architectural, mechanical, and electrical components (Simplified and Systematic Rehabilitation) - Report No. FEMA 274. In: *NEHRP Guidelines for the Seismic Rehabilitation of Buildings*. USA: Building Seismic Safety Council; 1997, pp. 11/1-11/48.

[9] Villaverde, R. Seismic Design of Secondary Structures: State of the Art. *Journal of Structural Engineering*, 1997, 123 (8), pp. 1011-1019. https://doi.org/10.1061/(ASCE)0733-9445(1997)123:8(1011)

[10] Villaverde, R. Simplified Seismic Analysis of Secondary Systems. *Journal of Structural Engineering*, 1986, 112 (3), pp. 588-604. https://doi.org/10.1061/(ASCE)0733-9445(1986)112:3(588)

[11] Villaverde, R. Simplified seismic analysis of piping or equipment mounted on two points of a multistory structure. *Nuclear Engineering and Design*, 1986, 92 (1), pp. 37-50. https://doi.org/10.1016/0029-5493(86)90097-X

[12] Villaverde, R. Simplified approach for the seismic analysis of equipment attached to elastoplastic structures. *Nuclear Engineering and Design*, 1987, 103 (3), pp. 267-279. https://doi.org/10.1016/0029-5493(87)90310-4

[13] Villaverde, R. Approximate formulas to calculate the seismic response of light attachments to buildings. *Nuclear Engineering and Design*, 1991, 128 (3), pp. 349-368. https://doi.org/10.1016/0029-5493(91)90172-E

[14] Adam, C. Dynamics of elastic-plastic frames with secondary structures: shake table and numerical studies. *Earthquake Engineering and Structural Dynamics*, 2001, 30 (2), pp. 257-277. https://doi.org/10.1002/1096-9845(200102)30:2%3C257::AID-EQE7%3E3.0.CO;2-J

[15] Filiatrault, A.; Sullivan, T. Performance-based seismic design of nonstructural building components: The next frontier of earthquake engineering. *Earthquake Engineering and Engineering Vibration*, 2014, 13 (Suppl. 1), pp. 17-46. https://doi.org/10.1007/s11803-014-0238-9

[16] Merino, R. J.; Perrone, D.; Filiatrault, A. Consistent floor response spectra for performance-based seismic design of nonstructural elements. *Earthquake Engineering & Structural Dynamics*, 2019, 49 (3), pp. 261-284. https://doi.org/10.1002/eqe.3236

[17] Surana, M. Evaluation of seismic design provisions for acceleration-sensitive nonstructural components. *Earthquakes and Structures*, 2019, 16 (5), pp. 611-623. https://doi.org/10.12989/eas.2019.16.5.611

[18] Ghafory-Ashtiani, M.; Fiouz, A. R. Response of secondary systems subjected to multicomponent earthquake. *Journal of Seismology and Earthquake Engineering*, 2004, 6 (2), pp. 29-45.

[19] Kazantzi, K.; Miranda, E.; Vamvatsikos, D. Strength-reduction factors for the design of light nonstructural elements in buildings. *Earthquake Engineering & Structural Dynamics*, 2020, 49 (13), pp. 1329-1343. https://doi.org/10.1002/eqe.3292

[20] Chalarcal, B.; Filiatrault, A; Perrone, D. Seismic demand on acceleration-sensitive nonstructural components in viscously damped braced frames. *Journal of Structural Engineering*, 2020, 146 (9). https://doi.org/10.1061/(ASCE)ST.1943-541X.0002770
[21] Torkian, Z.; Khodakarami, M. I. Development of Fragility Curves for Brick Infill Walls in Steel Frame Structures. *Journal of Rehabilitation in Civil Engineering*, 2022, 10 (4), pp. 45-55. https://doi.org/10.22075/jrce.2021.21646.1453
[22] Bagnoli, M.; Grande, E.; Milani, G. Reinforced Concrete Infilled Frames. *Encyclopedia*, 2022, 2 (1), pp. 473-485. https://doi.org/10.3390/encyclopedia2010030
[23] Sakcalı, G. B.; Öztürk, Y.; Çelik, İ. D.; Davraz, M. The effect of new generation polyurethane wall block on single span steel frame behavior. *Journal of Building Engineering*, 2022, 48, 103986. https://doi.org/10.1016/j.jobe.2021.103986
[24] Jagadeesan, P. et al. Study on Performance of Infilled Wall in an RC-Framed Structure Using a Reinforcing Band. *Advances in Materials Science and Engineering*, 2022, 2022 (1), 8643959. https://doi.org/10.1155/2022/8643959
[25] Wang, Z. et al. Out-of-plane performance of infilled frames with the improved flexible connection. *Journal of Building Engineering*, 2022, 51, 104286. https://doi.org/10.1016/j.jobe.2022.104286
[26] Asteris, P. G. Lateral stiffness of brick masonry infilled plane frames. *Journal of Structural Engineering*, 2003, 129 (8), pp. 1071-1079. https://doi.org/10.1061/(ASCE)0733-9445(2003)129:8(1071)
[27] Yekrangnia, M.; Asteris, P. G. Multi-strut macro-model for masonry infilled frames with openings. *Journal of Building Engineering*, 2020, 32, 101683. https://doi.org/10.1016/j.jobe.2020.101683
[28] Dias-Oliveira, J.; Rodrigues, H.; Asteris, P. G.; Varum, H. On the seismic behavior of masonry infilled frame structures. *Buildings*, 2022, 12 (8), 1146. https://doi.org/10.3390/buildings12081146
[29] Seismosoft. SeismoSignal - A computer program for signal processing of time-histories. Accessed: February 3, 2024. Available at: www.seismosoft.com
[30] Computers and Structures Inc. CSI. SAP2000 Integrated Software for Structural Analysis and Design. Accessed: February 3, 2024. Available at: https://www.csiamerica.com/products/sap2000
[31] Moeindarbari H.; Taghikhany T. Seismic optimum design of triple friction pendulum bearing subjected to near-fault pulse-like ground motions. *Structural and Multidisciplinary Optimization*, 2014, 50, pp. 701-716. https://doi.org/10.1007/s00158-014-1079-x